

Craig M Brown

List of Publications by Year in descending order

Source: <https://exaly.com/author-pdf/7007231/publications.pdf>

Version: 2024-02-01

239
papers

23,540
citations

16791

66
h-index

8878

150
g-index

247
all docs

247
docs citations

247
times ranked

23902
citing authors

#	ARTICLE	IF	CITATIONS
1	Neutron Vibrational Spectroscopic Evidence for Short H \cdots H Contacts in the $\text{Ni}_{1.4}\text{H}_{1.6}$ (Ce, La) Metal Hydride. <i>Neutron News</i> , 2022, 33, 7-9.	0.1	1
2	Stacking Faults Assist Lithium-Ion Conduction in a Halide-Based Superionic Conductor. <i>Journal of the American Chemical Society</i> , 2022, 144, 5795-5811.	6.6	50
3	Magnetic-Field-Induced Dielectric Anomalies in Cobalt-Containing Garnets. <i>Inorganic Chemistry</i> , 2022, 61, 5452-5458.	1.9	0
4	Lattice Dynamics in the NASICON $\text{NaZr}_2(\text{PO}_4)_3$ Solid Electrolyte from Temperature-Dependent Neutron Diffraction, NMR, and Ab Initio Computational Studies. <i>Chemistry of Materials</i> , 2022, 34, 4029-4038.	3.2	6
5	Turning Molecular Springs into Nano-Shock Absorbers: The Effect of Macroscopic Morphology and Crystal Size on the Dynamic Hysteresis of Water Intrusion into Hydrophobic Nanopores. <i>ACS Applied Materials & Interfaces</i> , 2022, 14, 26699-26713.	4.0	10
6	Polyoxocationic antimony oxide cluster with acidic protons. <i>Science Advances</i> , 2022, 8, .	4.7	5
7	Neutron scattering studies of materials for hydrogen storage. , 2021, , .		6
8	N e^{el} ordering in the distorted honeycomb pyrosilicate: $\text{Er}_2\text{Si}_2\text{O}_7$. <i>Journal of Physics Condensed Matter</i> , 2021, 33, 125804.	0.7	2
9	Ambient-Temperature Hydrogen Storage via Vanadium(II)-Dihydrogen Complexation in a Metal-Organic Framework. <i>Journal of the American Chemical Society</i> , 2021, 143, 6248-6256.	6.6	81
10	Compact Thermal Actuation by Water and Flexible Hydrophobic Nanopore. <i>ACS Nano</i> , 2021, 15, 9048-9056.	7.3	10
11	Spin Frustration in Double Perovskite Oxides and Oxynitrides: Enhanced Frustration in $\text{La}_2\text{MnTa}_5\text{N}$ with a Large Octahedral Rotation. <i>Inorganic Chemistry</i> , 2021, 60, 8252-8258.	1.9	7
12	Antiferromagnetic Order and Spin-Canting Transition in the Corrugated Square Net Compound $\text{Cu}_3(\text{TeO}_4)_2(\text{SO}_4)_2\text{H}_2\text{O}$. <i>Inorganic Chemistry</i> , 2021, 60, 10565-10571.	1.9	3
13	Magnetic structure, excitations and short-range order in honeycomb $\text{Na}_2\text{Ni}_2\text{TeO}_6$. <i>Journal of Physics Condensed Matter</i> , 2021, 33, 375803.	0.7	3
14	Spin Reorientation in Antiferromagnetic Layered FePt_5P . <i>ACS Applied Electronic Materials</i> , 2021, 3, 3501-3508.	2.0	8
15	Enhanced Magnetic Interaction by Face-Shared Hydride Anions in $6\text{H-BaCrO}_2\text{H}$. <i>Inorganic Chemistry</i> , 2021, 60, 11957-11963.	1.9	12
16	Observation of an Intermediate to H_2 Binding in a Metal-Organic Framework. <i>Journal of the American Chemical Society</i> , 2021, 143, 14884-14894.	6.6	32
17	The Rietveld Refinement Method: Half of a Century Anniversary. <i>Crystal Growth and Design</i> , 2021, 21, 4821-4822.	1.4	12
18	Magnetic properties and signatures of moment ordering in the triangular lattice antiferromagnet KCeO_2 . <i>Physical Review B</i> , 2021, 104, .	1.1	9

#	ARTICLE	IF	CITATIONS
19	Conduction Band Control of Oxyhalides with a Triple-Fluorite Layer for Visible Light Photocatalysis. <i>Journal of the American Chemical Society</i> , 2021, 143, 2491-2499.	6.6	52
20	Chemical Bonding Governs Complex Magnetism in MnPt_5P . <i>Inorganic Chemistry</i> , 2021, 60, 87-96.	1.9	9
21	Investigating the non-classical M-H ₂ bonding in $\text{OsClH}_3(\text{PPh}_3)_3$. <i>Journal of Alloys and Compounds</i> , 2021, 894, 162445.	2.8	1
22	Iridate Li_8IrO_6 : An Antiferromagnetic Insulator. <i>Inorganic Chemistry</i> , 2021, 60, 17201-17211.	1.9	1
23	Structural resolution and mechanistic insight into hydrogen adsorption in flexible ZIF-7. <i>Chemical Science</i> , 2021, 12, 15620-15631.	3.7	18
24	Physical properties of the quasi-two-dimensional square lattice antiferromagnet Ba_2O_7 . <i>Physical Review B</i> , 2021, 104, .	1.1	9
25	Efficient and tunable one-dimensional charge transport in layered lanthanide metal-organic frameworks. <i>Nature Chemistry</i> , 2020, 12, 131-136.	6.6	214
26	Strain-induced creation and switching of anion vacancy layers in perovskite oxynitrides. <i>Nature Communications</i> , 2020, 11, 5923.	5.8	20
27	Elucidating the Structure of the Metal-Organic Framework Ru-HKUST-1. <i>Chemistry of Materials</i> , 2020, 32, 7710-7715.	3.2	9
28	Dynamics of Hydroxyl Anions Promotes Lithium Ion Conduction in Antiperovskite Li_2OHCl . <i>Chemistry of Materials</i> , 2020, 32, 8481-8491.	3.2	53
29	Peritectic phase transition of benzene and acetonitrile into a cocrystal relevant to Titan, Saturn's moon. <i>Chemical Communications</i> , 2020, 56, 13520-13523.	2.2	11
30	Self-adjusting binding pockets enhance H_2 and CH_4 adsorption in a uranium-based metal-organic framework. <i>Chemical Science</i> , 2020, 11, 6709-6716.	3.7	25
31	Special section - Crystallography and properties of metal-organic framework (MOF) compounds. <i>Powder Diffraction</i> , 2020, 35, 2-2.	0.4	0
32	Negative cooperativity upon hydrogen bond-stabilized O_2 adsorption in a redox-active metal-organic framework. <i>Nature Communications</i> , 2020, 11, 3087.	5.8	36
33	Inter-Kramers Transitions and Spin-Phonon Couplings in a Lanthanide-Based Single-Molecule Magnet. <i>Inorganic Chemistry</i> , 2020, 59, 5218-5230.	1.9	25
34	Metastability and Reversibility of Anionic Redox-Based Cathode for High-Energy Rechargeable Batteries. <i>Cell Reports Physical Science</i> , 2020, 1, 100028.	2.8	37
35	Molecular Insight into Fluorocarbon Adsorption in Pore Expanded Metal-Organic Framework Analogs. <i>Journal of the American Chemical Society</i> , 2020, 142, 3002-3012.	6.6	44
36	Understanding How Ligand Functionalization Influences CO_2 and N_2 Adsorption in a Sodalite Metal-Organic Framework. <i>Chemistry of Materials</i> , 2020, 32, 1526-1536.	3.2	19


#	ARTICLE	IF	CITATIONS
37	Neutron diffraction structural study of CO ₂ binding in mixed-metal CPM-200 metal-organic frameworks. <i>Chemical Communications</i> , 2020, 56, 2574-2577.	2.2	5
38	Certification of Standard Reference Material 660c for powder diffraction. <i>Powder Diffraction</i> , 2020, 35, 17-22.	0.4	16
39	Competing antiferromagnetic-ferromagnetic states in a Kitaev honeycomb magnet. <i>Physical Review B</i> , 2020, 102, .	4.1	4
40	Long-range magnetic order in hydroxide-layer-doped (Li ^x Fe _{1-x} MnyOD)FeSe. <i>Physical Review Materials</i> , 2020, 4, .	0.9	3
41	Accessing New Charge-Transfer Complexes by Mechanochemistry: A Tetrathiafulvalene Chloranilic Acid Polymorph Containing Segregated Tetrathiafulvalene Stacks. <i>Crystal Growth and Design</i> , 2019, 19, 4970-4980.	1.4	6
42	Field-tunable quantum disordered ground state in the triangular-lattice antiferromagnet NaYbO ₂ . <i>Nature Physics</i> , 2019, 15, 1058-1064.	6.5	138
43	Dynamical Phase Transitions and Cation Orientation-Dependent Photoconductivity in CH(NH ₂) ₂ PbBr ₃ . , 2019, 1, 260-264.		35
44	Understanding Gas Storage in Cuboctahedral Porous Coordination Cages. <i>Journal of the American Chemical Society</i> , 2019, 141, 12128-12138.	6.6	73
45	Realization of interlayer ferromagnetic interaction in MnS ₂ . <i>Physical Review B</i> , 2019, 100, 104411.	1.1	81
46	Elusive Valence Transition in Mixed-Valence Sesquioxide Cs ₄ O ₆ . <i>Inorganic Chemistry</i> , 2019, 58, 14532-14541.	1.9	6
47	Correction to Dynamical Phase Transitions and Cation Orientation-Dependent Photoconductivity in CH(NH ₂) ₂ PbBr ₃ . , 2019, 1, 481-481.		0
48	Competing Polar and Antipolar Structures in the Ruddlesden-Popper Layered Perovskite Li ₂ SrNb ₂ O ₇ . <i>Chemistry of Materials</i> , 2019, 31, 4418-4425.	3.2	28
49	High-Pressure Synthesis of Non-Stoichiometric Li _x WO ₃ (0.5 ≤ x ≤ 1.0) with LiNbO ₃ Structure. <i>Inorganics</i> , 2019, 7, 63.	1.2	9
50	Rattling Behavior in a Simple Perovskite NaWO ₃ . <i>Inorganic Chemistry</i> , 2019, 58, 6790-6795.	1.9	9
51	Special section: crystallography and properties of metal organic framework (MOF) compounds. <i>Powder Diffraction</i> , 2019, 34, 2-2.	0.4	0
52	Probing Magnetic Excitations in Coll Single-Molecule Magnets by Inelastic Neutron Scattering. <i>European Journal of Inorganic Chemistry</i> , 2019, 2019, 1055-1055.	1.0	0
53	New insights into water dynamics of Portland cement paste with nano-additives using quasielastic neutron scattering. <i>Journal of Materials Science</i> , 2019, 54, 4710-4718.	1.7	3
54	Neutron Instruments for Research in Coordination Chemistry. <i>European Journal of Inorganic Chemistry</i> , 2019, 2019, 1065-1089.	1.0	29

#	ARTICLE	IF	CITATIONS
55	High-Pressure Synthesis of $A_2NiO_2Ag_2Se_2$ (A=Sr, Ba) with a High-Spin Ni^{2+} in Square-Planar Coordination. <i>Angewandte Chemie - International Edition</i> , 2019, 58, 756-759.	7.2	25
56	Probing Magnetic Excitations in Co^{II} Single-Molecule Magnets by Inelastic Neutron Scattering. <i>European Journal of Inorganic Chemistry</i> , 2019, 2019, 1119-1127.	1.0	14
57	An <i>In Situ</i> Neutron Diffraction and DFT Study of Hydrogen Adsorption in a Sodalite-Type Metal-Organic Framework, Cu_3T . <i>European Journal of Inorganic Chemistry</i> , 2019, 2019, 1147-1154.	1.0	15
58	Deciphering structural and magnetic disorder in the chiral skyrmion host materials Co_x		

#	ARTICLE	IF	CITATIONS
73	Record High Hydrogen Storage Capacity in the Metal-Organic Framework Ni ₂ (dobdc) at Near-Ambient Temperatures. Chemistry of Materials, 2018, 30, 8179-8189.	3.2	182
74	Defect-driven extreme magnetoresistance in an I-Mn-V semiconductor. Applied Physics Letters, 2018, 113, 122105.	1.5	6
75	Certification of Standard Reference Material 1879b respirable cristobalite. Powder Diffraction, 2018, 33, 202-208.	0.4	1
76	Gas adsorption in an isostructural series of pillared coordination cages. Chemical Communications, 2018, 54, 6392-6395.	2.2	19
77	Spin-phonon couplings in transition metal complexes with slow magnetic relaxation. Nature Communications, 2018, 9, 2572.	5.8	93
78	Methane Storage in Paddlewheel-Based Porous Coordination Cages. Journal of the American Chemical Society, 2018, 140, 11153-11157.	6.6	84
79	On the Structure-Property Relationships of Cation-Exchanged ZK5 Zeolites for CO ₂ Adsorption. ChemSusChem, 2017, 10, 946-957.	3.6	36
80	Performance of van der Waals Corrected Functionals for Guest Adsorption in the M ₂ (dobdc) Metal-Organic Frameworks. Journal of Physical Chemistry A, 2017, 121, 4139-4151.	1.1	41
81	Formation of [Cu ₂ O ₂] ²⁺ and [Cu ₂ O] ²⁺ toward C-H Bond Activation in Cu-SSZ-13 and Cu-SSZ-39. ACS Catalysis, 2017, 7, 4291-4303.	5.5	195
82	Metal-insulator transition tuned by magnetic field in Bi _{1.7} V ₈ O ₁₆ hollandite. Journal of Materials Chemistry C, 2017, 5, 4967-4976.	2.7	2
83	Reversible Capture and Release of Cl ₂ and Br ₂ with a Redox-Active Metal-Organic Framework. Journal of the American Chemical Society, 2017, 139, 5992-5997.	6.6	95
84	Selective Gas Adsorption in Highly Porous Chromium(II)-Based Metal-Organic Polyhedra. Chemistry of Materials, 2017, 29, 8583-8587.	3.2	68
85	Electronic Conductivity in a Porous Vanadyl Prussian Blue Analogue upon Air Exposure. Inorganic Chemistry, 2017, 56, 12682-12686.	1.9	13
86	Ising-like antiferromagnetism on the octahedral sublattice of a cobalt-containing garnet and the potential for quantum criticality. Physical Review B, 2017, 95, .	1.1	8
87	Combining microscopic and macroscopic probes to untangle the single-ion anisotropy and exchange energies in an $S=1$ quantum antiferromagnet. Physical Review B, 2017, 95, .	1.1	15
88	Cubic lead perovskite PbMoO ₃ with anomalous metallic behavior. Physical Review B, 2017, 95, .	1.1	13
89	Origin of long lifetime of band-edge charge carriers in organic-inorganic lead iodide perovskites. Proceedings of the National Academy of Sciences of the United States of America, 2017, 114, 7519-7524.	3.3	137
90	Pressure tuning of collapse of helimagnetic structure in $S=1$ AuMn ₂ Physical Review B, 2017, 96, .		

#	ARTICLE	IF	CITATIONS
91	Structural studies of small molecules adsorbed in MOFs. Acta Crystallographica Section A: Foundations and Advances, 2017, 73, C1031-C1031.	0.0	0
92	Hydrogen Storage and Selective, Reversible O ₂ Adsorption in a Metal-Organic Framework with Open Chromium(II) Sites. Angewandte Chemie - International Edition, 2016, 55, 8605-8609.	7.2	102
93	Hydrogen Storage and Selective, Reversible O ₂ Adsorption in a Metal-Organic Framework with Open Chromium(II) Sites. Angewandte Chemie, 2016, 128, 8747-8751.	1.6	23
94	Metastable Layered Cobalt Chalcogenides from Topochemical Deintercalation. Journal of the American Chemical Society, 2016, 138, 16432-16442.	6.6	61
95	Quasi-Elastic Neutron Scattering Studies of Hydrogen Dynamics for Nanoconfined NaAlH ₄ . Journal of Physical Chemistry C, 2016, 120, 14863-14873.	1.5	7
96	The magnetic transitions and dynamics in the multiferroic Lu _{0.5} Sc _{0.5} FeO ₃ . MRS Advances, 2016, 1, 565-571.	0.5	4
97	High Thermopower with Metallic Conductivity in <i>p</i> -Type Li-Substituted PbPdO ₂ . Chemistry of Materials, 2016, 28, 3367-3373.	3.2	25
98	Outlook and challenges for hydrogen storage in nanoporous materials. Applied Physics A: Materials Science and Processing, 2016, 122, 1.	1.1	129
99	The low-temperature structural behavior of sodium 1-carba-closo-decaborate: NaCB ₉ H ₁₀ . Journal of Solid State Chemistry, 2016, 243, 162-167.	1.4	12
100	Strong correlations between vacancy and magnetic ordering in superconducting K _{0.8} Fe ₂ As ₂ . Physical Review B, 2016, 94, .	1.1	4
101	ZnTaO ₂ N: Stabilized High-Temperature LiNbO ₃ -type Structure. Journal of the American Chemical Society, 2016, 138, 15950-15955.	6.6	26
102	Physical properties of the Ce ₂ MAl ₇ Ge ₄ heavy-fermion compounds (M=Co, Ir, Ni, Pd). Physical Review B, 2016, 93, .	1.1	8
103	High-Pressure Synthesis of Manganese Oxyhydride with Partial Anion Order. Angewandte Chemie - International Edition, 2016, 55, 9667-9670.	7.2	31
104	Local Jahn-Teller distortions and orbital ordering in Ba ₃ Cu _{1+x} Sb ₂ As ₉ investigated by neutron scattering. Physical Review B, 2016, 93, .	1.1	4
105	Hydration-induced spin-glass state in a frustrated Na-Mn-O triangular lattice. Physical Review B, 2016, 93, .	1.1	11
106	Entropy-driven structural transition and kinetic trapping in formamidinium lead iodide perovskite. Science Advances, 2016, 2, e1601650.	4.7	203
107	Three-dimensional protonic conductivity in porous organic cage solids. Nature Communications, 2016, 7, 12750.	5.8	133
108	Tuning the Adsorption-Induced Phase Change in the Flexible Metal-Organic Framework Co(bdp). Journal of the American Chemical Society, 2016, 138, 15019-15026.	6.6	123

#	ARTICLE	IF	CITATIONS
109	Adsorption of two gas molecules at a single metal site in a metal-organic framework. <i>Chemical Communications</i> , 2016, 52, 8251-8254.	2.2	45
110	Water dynamics in cement paste at early age prepared with pozzolanic volcanic ash and Ordinary Portland Cement using quasielastic neutron scattering. <i>Cement and Concrete Research</i> , 2016, 86, 55-62.	4.6	29
111	Dynamics of Pyramidal SiH_3^+ Ions in ASiH_3 (A = K and Rb) Investigated with Quasielastic Neutron Scattering. <i>Journal of Physical Chemistry C</i> , 2016, 120, 6369-6376.	1.5	17
112	Improved Catalytic Activity and Stability of a Palladium Pincer Complex by Incorporation into a Metal-Organic Framework. <i>Journal of the American Chemical Society</i> , 2016, 138, 1780-1783.	6.6	141
113	Topochemical Nitridation with Anion Vacancy-Assisted $\text{N}_3^-/\text{O}^{2-}$ Exchange. <i>Journal of the American Chemical Society</i> , 2016, 138, 3211-3217.	6.6	47
114	Hydrogen Storage in the Expanded Pore Metal-Organic Frameworks $\text{M}_2(\text{dobpc})$ (M = Mg, Tj) <i>ETQ</i> 0.0 0 rgBT/Overlock	3.2	171
115	MnTaO_2N : Polar LiNbO_3 -type Oxynitride with a Helical Spin Order. <i>Angewandte Chemie - International Edition</i> , 2015, 54, 516-521.	7.2	39
116	Observation of drastic change of generalized phonon density-of-states in nanostructured half-Heusler using inelastic neutron scattering. <i>Applied Physics Letters</i> , 2015, 107, 213901.	1.5	3
117	Adsorption of hydrocarbons in the porous borohydride framework $\text{Mg}(\text{BH}_4)_2$. <i>Acta Crystallographica Section A: Foundations and Advances</i> , 2015, 71, s275-s275.	0.0	0
118	Understanding Small-Molecule Interactions in Metal-Organic Frameworks: Coupling Experiment with Theory. <i>Advanced Materials</i> , 2015, 27, 5785-5796.	11.1	33
119	Oxygen interstitials and vacancies in $\text{LaSrGa}_3\text{O}_7$ -based melilites. <i>Journal of Solid State Chemistry</i> , 2015, 230, 309-317.	1.4	20
120	Magnetic Structure and Exchange Interactions in Quasi-One-Dimensional $\text{MnCl}_2(\text{urea})_2$. <i>Inorganic Chemistry</i> , 2015, 54, 11897-11905.	1.9	20
121	Inducing Ferrimagnetism in Insulating Hollandite $\text{Ba}_{1.2}\text{Mn}_8\text{O}_{16}$. <i>Chemistry of Materials</i> , 2015, 27, 515-525.	3.2	22
122	Gradual Release of Strongly Bound Nitric Oxide from $\text{Fe}_2(\text{NO})_2$ (dobdc). <i>Journal of the American Chemical Society</i> , 2015, 137, 3466-3469.	6.6	81
123	Flexible metal-organic framework compounds: In situ studies for selective CO_2 capture. <i>Journal of Alloys and Compounds</i> , 2015, 647, 24-34.	2.8	25
124	Stabilization of cubic $\text{Sr}_2\text{FeMoO}_6$ through topochemical reduction. <i>Chemical Communications</i> , 2015, 51, 12201-12204.	2.2	9
125	Methane storage in flexible metal-organic frameworks with intrinsic thermal management. <i>Nature</i> , 2015, 527, 357-361.	13.7	817
126	Rotational dynamics of organic cations in the $\text{CH}_3\text{NH}_3\text{PbI}_3$ perovskite. <i>Physical Chemistry Chemical Physics</i> , 2015, 17, 31278-31286.	1.3	212

#	ARTICLE	IF	CITATIONS
127	A labile hydride strategy for the synthesis of heavily nitrized BaTiO ₃ . Nature Chemistry, 2015, 7, 1017-1023.	6.6	118
128	Critical Factors Driving the High Volumetric Uptake of Methane in Cu ₃ (btc) ₂ . Journal of the American Chemical Society, 2015, 137, 10816-10825.	6.6	73
129	Evolution of magnetism in the 		

#	ARTICLE	IF	CITATIONS
145	Chemical spectroscopy using neutrons. Chemical Physics, 2013, 427, 1-2.	0.9	2
146	Structure and spectroscopy of hydrogen adsorbed in a nickel metal-organic framework. Chemical Physics, 2013, 427, 3-8.	0.9	23
147	Selective adsorption of ethylene over ethane and propylene over propane in the metal-organic frameworks M2(dobdc) (M = Mg, Mn, Fe, Co, Ni, Zn). Chemical Science, 2013, 4, 2054.	3.7	398
148	Mn(dca)2(o-phen) {dca=dicyanamide; o-phen=1,10-phenanthroline}: Long-range magnetic order in a low-dimensional Mn-dca polymer. Polyhedron, 2013, 52, 679-688.	1.0	8
149	Noble Gas Adsorption in Copper Trimesate, HKUST-1: An Experimental and Computational Study. Journal of Physical Chemistry C, 2013, 117, 20116-20126. Muon spin relaxation and electron/neutron diffraction studies of BaTi	1.5	92

150

#	ARTICLE	IF	CITATIONS
163	Neutron Scattering and Spectroscopic Studies of Hydrogen Adsorption in Cr ₃ (BTC) ₂ —A Metal—Organic Framework with Exposed Cr ²⁺ Sites. Journal of Physical Chemistry C, 2011, 115, 8414-8421.	1.5	50
164	Hydrogen storage properties and neutron scattering studies of Mg ₂ (dobdc)—a metal—organic framework with open Mg ²⁺ adsorption sites. Chemical Communications, 2011, 47, 1157-1159.	2.2	178
165	Selective Binding of O ₂ over N ₂ in a Redox—Active Metal—Organic Framework with Open Iron(II) Coordination Sites. Journal of the American Chemical Society, 2011, 133, 14814-14822.	6.6	470
166	Micro-channel development and hydrogen adsorption properties in templated microporous carbons containing platinum nanoparticles. Carbon, 2011, 49, 1305-1317.	5.4	30
167	Low-energy magnetic excitations in Co/CoO core/shell nanoparticles. Physical Review B, 2011, 83, .	1.1	18
168	Hydrogen storage and carbon dioxide capture in an iron-based sodalite-type metal—organic framework (Fe-BTT) discovered via high-throughput methods. Chemical Science, 2010, 1, 184.	3.7	294
169	Identifying the Specific Nanostructures Responsible for the High Thermoelectric Performance of (Bi,Sb) ₂ Te ₃ Nanocomposites. Nano Letters, 2010, 10, 3283-3289.	4.5	484
170	Metal—Organic Frameworks with Exceptionally High Methane Uptake: Where and How is Methane Stored?. Chemistry - A European Journal, 2010, 16, 5205-5214.	1.7	227
171	Highly-Selective and Reversible O ₂ Binding in Cr ₃ (1,3,5-benzenetricarboxylate) ₂ . Journal of the American Chemical Society, 2010, 132, 7856-7857.	6.6	307
172	DAVE: A Comprehensive Software Suite for the Reduction, Visualization, and Analysis of Low Energy Neutron Spectroscopic Data. Journal of Research of the National Institute of Standards and Technology, 2009, 114, 341.	0.4	786
173	User Facilities: The Education of New Neutron Users. , 2009, , .		1
174	Adsorption and melting of hydrogen in potassium-intercalated graphite. Physical Review B, 2009, 79, .	1.1	32
175	Neutron scattering evidence for isolated spin-1 ladders in (C ₅ D ₁₂ N) ₂ CuBr ₄ . Physical Review B, 2009, 80, .	1.1	31
176	Hydrogen adsorption in HKUST-1: a combined inelastic neutron scattering and first-principles study. Nanotechnology, 2009, 20, 204025.	1.3	112
177	One-Dimensional Magnetic Fluctuations in the Spin-2 Triangular Lattice—NaMnO ₂ . Physical Review Letters, 2009, 103, 077202.	2.9	63
178	Detection of Hydrogen Spillover in Palladium-Modified Activated Carbon Fibers during Hydrogen Adsorption. Journal of Physical Chemistry C, 2009, 113, 5886-5890.	1.5	151
179	Role of Cation Size on the Structural Behavior of the Alkali-Metal Dodecahydro-Dodecaborates. Journal of Physical Chemistry C, 2009, 113, 11187-11189.	1.5	55
180	High Capacity Hydrogen Adsorption in Cu(II) Tetracarboxylate Framework Materials: The Role of Pore Size, Ligand Functionalization, and Exposed Metal Sites. Journal of the American Chemical Society, 2009, 131, 2159-2171.	6.6	723

#	ARTICLE	IF	CITATIONS
181	Neutron powder diffraction of metal-organic frameworks for hydrogen storage. <i>Pramana - Journal of Physics</i> , 2008, 71, 755-760.	0.9	17
182	The design of a bismuth-based auxiliary filter for the removal of spurious background scattering associated with filter-analyzer neutron spectrometers. <i>Nuclear Instruments and Methods in Physics Research, Section A: Accelerators, Spectrometers, Detectors and Associated Equipment</i> , 2008, 588, 406-413.	0.7	69
183	Quasielastic neutron scattering of NH_3 and BH_3 rotational dynamics in orthorhombic ammonia borane. <i>Chemical Physics Letters</i> , 2008, 459, 85-88.	1.2	27
184	Reversible Structural Transition in MIL-53 with Large Temperature Hysteresis. <i>Journal of the American Chemical Society</i> , 2008, 130, 11813-11818.	6.6	402
185	Hydrogen Adsorption in a Highly Stable Porous Rare-Earth Metal-Organic Framework: Sorption Properties and Neutron Diffraction Studies. <i>Journal of the American Chemical Society</i> , 2008, 130, 9626-9627.	6.6	294
186	Inelastic neutron scattering from confined molecular oxygen. <i>Physical Review B</i> , 2008, 78, .	1.1	10
187	Increasing the Density of Adsorbed Hydrogen with Coordinatively Unsaturated Metal Centers in Metal-Organic Frameworks. <i>Langmuir</i> , 2008, 24, 4772-4777.	1.6	258
188	Crystalline Electric Field as a Probe for Long-Range Antiferromagnetic Order and Superconducting State of $\text{CeFeAsO}_{1-x}\text{F}_x$. <i>Physical Review Letters</i> , 2008, 101, 217002.	1.9	56
189	Neutron scattering studies on deuterium-adsorbed pore framework compound, $\text{K}_2\text{Zn}_3[\text{Fe}(\text{CN})_6]_2$. <i>Acta Crystallographica Section A: Foundations and Advances</i> , 2008, 64, C84-C84.	0.3	0
190	Inelastic neutron scattering study of hydrogen in $\text{d}_8\text{-THF} \cdot \text{D}_2\text{O}$ ice clathrate. <i>Journal of Chemical Physics</i> , 2007, 127, 134505.	1.2	32
191	Structural Characterization of D_2 in $\text{Cu}_3(1,3,5\text{-Benzenetricarboxylate})_2$ Using Neutron Powder Diffraction. <i>Materials Science Forum</i> , 2007, 561-565, 1601-1604.	0.3	2
192	Hydrogen Adsorption in MOF-74 Studied by Inelastic Neutron Scattering. <i>Materials Research Society Symposia Proceedings</i> , 2007, 1041, 1.	0.1	1
193	Neutron vibrational spectroscopy of the $\text{Pr}_2\text{Fe}_{17}$ -based hydrides. <i>Journal of Alloys and Compounds</i> , 2007, 446-447, 504-507.	2.8	6
194	Inelastic neutron scattering of H_2 adsorbed in HKUST-1. <i>Journal of Alloys and Compounds</i> , 2007, 446-447, 385-388.	2.8	74
195	Inelastic neutron scattering of H_2 adsorbed on boron substituted single walled carbon nanotubes. <i>Journal of Alloys and Compounds</i> , 2007, 446-447, 368-372.	2.8	16
196	Dynamics and Structure of Hydration Water on Rutile and Cassiterite Nanopowders Studied by Quasielastic Neutron Scattering and Molecular Dynamics Simulations. <i>Journal of Physical Chemistry C</i> , 2007, 111, 4328-4341.	1.5	132
197	Observation of Cu^{2+} - H_2 Interactions in a Fully Desolvated Sodalite-Type Metal-Organic Framework. <i>Angewandte Chemie - International Edition</i> , 2007, 46, 1419-1422.	7.2	395
198	Neutron Powder Diffraction Study of D_2 Sorption in $\text{Cu}_3(1,3,5\text{-benzenetricarboxylate})_2$. <i>Journal of the American Chemical Society</i> , 2006, 128, 15578-15579.	6.6	266

#	ARTICLE	IF	CITATIONS
199	Quasielastic and inelastic neutron scattering study of the hydration of monoclinic and triclinic tricalcium silicate. <i>Chemical Physics</i> , 2006, 326, 381-389.	0.9	17
200	Inelastic neutron scattering from antiferromagnetically coupled nearest-neighbor spin pairs in Zn(Mn)O and Zn(Mn)Te. <i>Physica B: Condensed Matter</i> , 2006, 385-386, 388-390.	1.3	1
201	Hydrogen Storage in a Microporous Metal-Organic Framework with Exposed Mn ²⁺ Coordination Sites. <i>Journal of the American Chemical Society</i> , 2006, 128, 16876-16883.	6.6	1,081
202	Dynamics of ammonia borane using neutron scattering. <i>Physica B: Condensed Matter</i> , 2006, 385-386, 266-268.	1.3	23
203	Determination of antiferromagnetic interactions in Zn(Mn)O, Zn(Co)O, and Zn(Mn)Te by inelastic neutron scattering. <i>Journal of Applied Physics</i> , 2006, 99, 08M122.	1.1	11
204	Static and dynamic Jahn-Teller effect in the alkali metal fulleride salts A ₄ C ₆₀ (A=K,Rb,Cs). <i>Physical Review B</i> , 2006, 73, .	1.1	33
205	Origin and removal of spurious background peaks in vibrational spectra measured by filter-analyzer neutron spectrometers. <i>Nuclear Instruments and Methods in Physics Research, Section A: Accelerators, Spectrometers, Detectors and Associated Equipment</i> , 2004, 517, 189-201.	0.7	52
206	Determination of hole-induced ferromagnetic exchange between nearest-neighbor Mn spins in p-type Zn _{1-x} Mn _x Te. <i>Journal of Magnetism and Magnetic Materials</i> , 2004, 272-276, E1545-E1546.	1.0	0
207	Determination of hole-induced ferromagnetic Mn-Mn exchange in p-type Zn _{1-x} Mn _x Te by inelastic neutron scattering. <i>Physica B: Condensed Matter</i> , 2004, 350, 36-39.	1.3	3
208	The Crystalline Enol of 1,3-Cyclohexanedione and Its Complex with Benzene: Vibrational Spectra, Simulation of Structure and Dynamics and Evidence for Cooperative Hydrogen Bonding. <i>Journal of Physical Chemistry A</i> , 2004, 108, 7356-7363.	1.1	14
209	Investigation of the State of Water in Hydrating Layered Sodium Disilicate in Crystalline and Amorphous Forms by Quasi-Elastic Neutron Scattering. <i>Chemistry of Materials</i> , 2004, 16, 5042-5050.	3.2	14
210	Dynamics of supercooled water in mesoporous silica matrix MCM-48-S. <i>European Physical Journal E</i> , 2003, 12, 59-62.	0.7	14
211	Terahertz spectroscopy of short-chain polypeptides. <i>Chemical Physics Letters</i> , 2003, 375, 337-343.	1.2	144
212	Structure and dynamics of superconducting Na _x CoO ₂ hydrate and its unhydrated analog. <i>Physical Review B</i> , 2003, 68, .	1.1	106
213	Comparison of Boson Peaks in Polypropylenes. <i>Macromolecules</i> , 2003, 36, 520-521.	2.2	0
214	Probing Hole-Induced Ferromagnetic Exchange in Magnetic Semiconductors by Inelastic Neutron Scattering. <i>Physical Review Letters</i> , 2003, 91, 087205.	2.9	54
215	Rotational dynamics of hydration water in dicalcium silicate by quasielastic neutron scattering. <i>Physical Review E</i> , 2002, 65, 040501.	0.8	34
216	Probing Vibrational Dynamics of Hydrogen-Bonded Inclusion Compounds with Inelastic Neutron Scattering and Ab Initio Calculations. <i>Journal of Physical Chemistry B</i> , 2002, 106, 4916-4924.	1.2	7

#	ARTICLE	IF	CITATIONS
217	Solid-State Ligand Dynamics in Interpenetrating Mn[N(CN) ₂] ₂ (Pyrazine): A Neutron Spectroscopy Study. <i>Journal of the American Chemical Society</i> , 2002, 124, 12600-12605.	6.6	19
218	Giant Anharmonicity and Nonlinear Electron-Phonon Coupling in MgB ₂ : A Combined First-Principles Calculation and Neutron Scattering Study. <i>Physical Review Letters</i> , 2001, 87, 037001.	2.9	381
219	Incoherent Quasi-elastic Neutron Scattering from Fructose-Water Solutions. <i>Journal of Physical Chemistry B</i> , 2001, 105, 7799-7804.	1.2	19
220	Muon-spin-rotation and magnetization study of metal-organic magnets based on the dicyanamide anion. <i>Journal of Physics Condensed Matter</i> , 2001, 13, 2263-2270.	0.7	9
221	Large Harmonic Softening of the Phonon Density of States of Uranium. <i>Physical Review Letters</i> , 2001, 86, 3076-3079.	2.9	76
222	Quantum rotation of hydrogen in single-wall carbon nanotubes. <i>Chemical Physics Letters</i> , 2000, 329, 311-316.	1.2	128
223	A view of dynamics changes in the molten globule-native folding step by quasielastic neutron scattering 1 Edited by P. E. Wright. <i>Journal of Molecular Biology</i> , 2000, 301, 525-536.	2.0	58
224	Powder diffraction and inelastic neutron scattering studies of the Na ₂ RbC ₆₀ fulleride. <i>Journal of Materials Chemistry</i> , 2000, 10, 1443-1449.	6.7	3
225	Anomalous High Pressure Properties in Fullerene Superconductors. <i>Molecular Crystals and Liquid Crystals</i> , 2000, 340, 599-604.	0.3	2
226	Neutron diffraction study of the polymeric structure of. <i>Journal of Physics Condensed Matter</i> , 1999, 11, 371-381.	0.7	11
227	Pressure dependence of superconductivity in the Na ₂ Rb _{0.5} Cs _{0.5} C ₆₀ fulleride. <i>Physical Review B</i> , 1999, 59, 4439-4444.	1.1	22
228	Rotational tunneling of ammonia in (NH ₃)K ₃ C ₆₀ . <i>Journal of Chemical Physics</i> , 1999, 111, 10969-10973.	1.2	1
229	Structural and Electronic Properties of the Noncubic Superconducting Fullerenes A ₄ C ₆₀ (A = Ba, Sr). <i>Physical Review Letters</i> , 1999, 83, 2258-2261.	2.9	36
230	Superconductivity in Li _x CsC ₆₀ fullerenes. <i>Physical Review B</i> , 1999, 59, R6628-R6630.	1.1	50
231	Pressure and Temperature Evolution of the Structure of the Superconducting Na ₂ CsC ₆₀ Fulleride. <i>Journal of Solid State Chemistry</i> , 1999, 145, 471-478.	1.4	23
232	Temperature and pressure dependence of orientational disorder and bonding in Li ₂ CsC ₆₀ . <i>Solid State Sciences</i> , 1999, 1, 157-163.	0.8	3
233	Band filling and width control in fullerenes. <i>Synthetic Metals</i> , 1999, 103, 2462-2465.	2.1	0
234	Current Issues of Intercalation and Superconductivity in Solid State Fullerenes, Nanotubes, and Carbon Nanostructures, 1999, 7, 587-598.	0.6	2

#	ARTICLE	IF	CITATIONS
235	Crystal Structure of the Higher Fullerene C84. Chemistry of Materials, 1998, 10, 1742-1744.	3.2	31
236	Fulleride polymerisation at ambient and elevated pressure. , 1998, , .		0
237	Effects of Pressure on the Azafullerene (C59N)2Molecular Solid to 22 GPa. Journal of the American Chemical Society, 1996, 118, 8715-8716.	6.6	42
238	On the Crystal Structure of Azafullerene (C59N)2. Chemistry of Materials, 1996, 8, 2548-2550.	3.2	52
239	Interfullerene vibrations in the polymeric fulleride CsC60. Chemical Communications, 1996, , 2465.	2.2	6